ORIGINAL PAPER

Aberrant Intrinsic Brain Activity in Patients with Autism Spectrum Disorder: Insights from EEG Microstates

Huibin Jia[1] · Dongchuan Yu[1]

Abstract

Autism spectrum disorder (ASD) involves aberrant organization and functioning of large-scale brain networks. The aim of this study was to examine whether the resting-state EEG microstate analysis could provide novel insights into the abnormal temporal and spatial properties of intrinsic brain activities in patients with ASD. To achieve this goal, EEG microstate analysis was conducted on the resting-state EEG datasets of 15 patients with ASD and 18 healthy controls from the Healthy Brain Network. The parameters (i.e., duration, occurrence rate, time coverage and topographical configuration) of four classical microstate classes (i.e., class A, B, C and D) were statistically tested between two groups. The results showed that: (1) the occurrence rate and time coverage of microstate class B in ASD group were significantly larger than those in control group; (2) the duration of microstate class A, the duration and time coverage of microstate class C were significantly smaller than those in control group; (3) the map configuration and occurrence rate differed significantly between two groups for microstate class D. These results suggested that EEG microstate analysis could be used to detect the deviant functions of large-scale cortical activities in ASD, and may provide indices that could be used in clinical researches of ASD.

Keywords Microstates parameter · Resting-state network · Phonological processing · Self-representation

Introduction

Autism spectrum disorder (ASD) could affect the developmental trajectory in several key cognitive and behavioral domains, such as social interaction and language abilities (Woolfenden et al. 2012). Recently, researchers have got a deep understanding of the biological mechanisms that underpin this disorder through neuroimaging of brain structure and of brain activity (Parellada et al. 2014). Studies suggested that brain abnormalities in ASD are not confined to any particular brain region, which has been revealed in numerous studies (Just et al. 2012). Abnormal brain activities more likely occur in distributed brain networks, such as the default mode network and language-related network

✉ Dongchuan Yu
  dcyu@seu.edu.cn

[1] Key Laboratory of Child Development and Learning Science of Ministry of Education, Research Center for Learning Science, School of Biological Sciences & Medical Engineering, Southeast University, Nanjing, Jiangsu, China

(Jung et al. 2014; Just et al. 2004). Aberrant temporal and spatial properties of these brain networks are key characteristics of ASD, which could interpret the diverse symptoms of ASD to some extent (Chen et al. 2017; Falahpour et al. 2016). Instead of investigating the abnormal activities of specific cortical regions, studying the aberrant organization and functioning of large-scale neural networks should provide more insights regarding the neurobiology of ASD.

The functional magnetic resonance imaging (fMRI) can be used to detect the properties of large-scale cortical networks, due to its excellent spatial resolution. However, the temporal resolution of fMRI is too poor to assess the activation timing of these networks. The electroencephalogram (EEG) which has outstanding temporal resolution (~ 1 ms) can also be used to investigate the functions of large-scale cortical networks. Of all the quantitative EEG techniques, EEG microstate analysis is one of the whole-brain imaging approaches that could characterize the spatial organization and temporal dynamics of large-scale cortical activities with high temporal resolution (Michel and Koenig 2018). The concept "EEG microstate" comes from the finding that broad-band spontaneous EEG activity at rest can be described by a limited number of scalp potential

topographies that remain quasi-stable for certain length of time (~ 60 to 120 ms) before rapidly changing into a new map configuration that remains stable again (Gao et al. 2017). These quasi-stable periods, which occur at a rate compatible with the speed of human information processing, are called "microstates" (Van de Ville et al. 2010). Using modified pattern classification algorithms, four microstate classes (labeled as class A, B, C and D), which could explain about 80% of the total EEG data variance, have been consistently identified in different studies with notable similarity across subjects (Andreou et al. 2014; Van de Ville et al. 2010). Britz et al. (2010) indicated that they were closely related with some large-scale resting-state networks obtained from the blood oxygen level dependent (BOLD) signal (Britz et al. 2010). Note that, although these two phenomena are closely linked, they may not reflect exactly the same kinds of cortical activities, which needs further investigation. Previous studies revealed that their parameters (e.g., duration, occurrence rate, and time coverage) were modulated by neuropsychiatric disorders, age, personality differences and cognitive manipulations (Koenig et al. 2002; Rieger et al. 2016; Schlegel et al. 2012; Seitzman et al. 2017).

To our knowledge no study to date has attempt to investigate whether the EEG microstate analysis could provide biomarkers in ASD researches. The goal of the current study was to examine the EEG microstate properties in patients with ASD using the resting-state EEG datasets of the Healthy Brain Network (HBN), which is an ongoing initiative focused on creating and sharing a biobank comprised of data from New York City area children and adolescents (Alexander et al. 2017). We hypothesized that the spatial and temporal properties of certain microstates (e.g., phonological processing related class A and self-representation related class C) may be altered in patients with ASD.

Materials and Methods

Participants

The resting-state EEG data of 15 right-handed male patients with ASD (mean age = 11.6 years, SD = 4.4 years; aged from 5 to 18 years) and 18 healthy male controls (mean age = 8.9 years, SD = 2.4 years; aged from 5 to 15 years) were selected. The selection of participants is based on the following criteria: (1) aged between 5 and 18 years; (2) male; (3) right-handed according to the Edinburgh Handedness Inventory (Oldfield 1971); (4) they were willing to participate in the EEG recording; (5) the EEG recording was successfully completed; (6) the EEG data have relatively high signal-to-noise ratio (SNR). The EEG signals were carefully inspected by two technicians who were familiar with EEG signals processing. The EEG datasets with too many bad

channels (> 20) and large drift for most of the recording time (> 50%) were deemed as EEG datasets with low SNR; (7) the participants in the ASD group were diagnosed with ASD by clinical team based on computerized web-based version of the Schedule for Affective Disorders and Schizophrenia—Children's version (Kaufman et al. 1997) and Autism Diagnostic Observation Schedule (ADOS) (Lord et al. 2012). All these patients were high-function autism (i.e., IQ > 66). The difference between IQs of the two groups did not reach significant level ($p > 0.05$).

Participants with cognitive or behavioral impairments, history of certain neurological diseases, substance dependence that could interfere with participation and confound brain-related findings have been excluded in EEG data recording (Alexander et al. 2017). For all the 15 patients with ASD, 2 patients were diagnosed with ASD for the first time (i.e., during the data collection of the HBN initiative). Participants taking stimulant medication were asked to discontinue their medication during the days of participation, as stimulants are known to have an effect on cognitive and behavioral testing, as well as functional brain mapping. None of the children in the ASD group has ever been diagnosed with the comorbidity of attention-deficit/hyperactivity disorder (ADHD).

The study was approved by the Chesapeake Institutional Review Board (https://www.chesapeakeirb.com/), and was conducted in accordance with the Declaration of Helsinki. Written consent were obtained from their legal guardians and written assent obtained from the participants.

EEG Recording

During EEG recording, the participants were asked to view a fixation cross in the center of computer screen, and were instructed to open or close their eyes at various time points.

About 5 min EEG data were recorded in a sound- and electrically-shielded room using a 128-channel Hydro-Cel Geodesic (EGI Inc., Eugene, Oregon, USA) system. EEG data were referenced to electrode Cz (vertex of the head). All electrode impedances were kept lower than 40 kΩ. Signals were amplified and digitized using a sampling rate of 500 Hz, and band-pass filtered between 0.1 and 100 Hz during recording.

EEG Data Preprocessing

EEG data were pre-processed using EEGLAB (Delorme and Makeig 2004). The EEG data preprocessing consisted of the following steps: (1) electrodes located on the neck/face were removed; (2) data portions with large drift were removed; (3) channels with bad activation were interpolated using a spherical spline method; (4) continuous EEG data were band-pass filtered between 0.5 and 80 Hz; (5) a notch

filter was used to eliminate 60 Hz line noise; (6) data portions contaminated by eye movements and blinks, electromyography, electrocardiography or any non-physiological artifacts were corrected using independent component analysis (ICA); (7) the continuous EEG data were remontaged against average reference, and segmented into 2000 ms epochs; (8) EEG epochs with amplitude values exceeding ± 80 µV at any electrode were rejected.

Note that observing the activations, scalp map and power spectrum of each independent component (IC), we could find many artifacts-related ICs do not have any physiological origin. One kind of "non-physiological artifacts" which could be found in many datasets has the following characters: (1) during certain time segments we could observe large drift, whereas the amplitude of this component is very small over other time segments; (2) observing the scalp map of this IC, we could find that this IC is only closely associated with one certain channel.

For the ASD group, the numbers of eyes open epochs and eyes closed epochs (mean $\pm$ SD) are 40.4 ± 8 and 47.9 ± 15.3 respectively. For the TD group, the numbers of eyes open epochs and eyes closed epochs (mean $\pm$ SD) are 41.9 ± 8.8 and 43.2 ± 13.2 respectively. The number of remaining epochs (either eyes open epochs or eyes closed epochs) did not differ significantly between two groups ($ps > 0.05$).

EEG Microstate Analysis

Before microstate analysis, the remained EEG epochs were digitally band-pass filtered between 2 and 20 Hz as suggested by previous studies (Lehmann et al. 2005; Schlegel et al. 2012). The microstate analysis was conducted on the whole EEG signals composed by mixed eye-open and eye-closed time periods.

Here, the microstate analyses were based on the Topographic Atomize & Agglomerate Hierarchical Clustering (T-AAHC) algorithm. More information about this algorithm can be found in other literatures (Brunet et al. 2010; Santarnecchi et al. 2017). Many approaches exist in the spatial analysis of EEG/ERP signals. Apart from the T-AAHC method, the modified k-means clustering analysis, proposed by Pascual-Marqui et al. (1995), is a classical method that has been used in many studies (Pascual-Marqui et al. 1995). However, since this k-means clustering method is based on the random selection of topographies from the dataset being analyzed as seed clusters, its results can in principle vary from one run to the next, even though the same dataset is being analyzed. This can be solved through a high number of randomizations, which will drastically increase the computational time. However, the T-AAHC which operates in a bottom-up manner wherein the number of clusters is initially large and progressively diminishes could drastically reduce

the computational efforts (Brunet et al. 2010). For these reasons, the T-AAHC algorithm is used in current study.

For the current datasets, the microstate analyses consist of the following steps. Firstly, the topographies of prepossessed EEG data of each subject are submitted to the T-AAHC algorithm, which could identify clusters with similar topographical configurations. Here, the polarity of each map is disregarded. Each of the resulting clusters represents one microstate class. Secondly, we used the criteria implemented in Cartool (i.e., Davies & Bouldin, Gamma, Silhouette, Dunn Robust, Point-Biserial, Krzanowski-Lai Index, and Cross-Validation) to determine the optimal number of clusters in the individual level and group level. The Cartool (https://sites.google.com/site/cartoolcommunity/) is a free software which was developed by the Functional Brain Mapping Laboratory in University of Geneva and could be used to perform EEG/ERP microstate analysis (Brunet et al. 2010). The order of microstate classes was determined by the spatial correlation between the topographical maps of group-level microstate classes. Finally, each original map was assigned to one of the EEG microstates using maximum spatial correlation coefficient between the tested original map and the group-level microstate maps as a criterion. As a result, each epoch was re-expressed as an alternating sequence of microstates. During this procedure, a temporal smoothing (window half-size 30 ms), Besag factor of 10 and a rejection of small time frames (when < 30 ms) was applied (Murray et al. 2008). The microstate sequence of a representative epoch is shown in Fig. 1.

Microstate Parameters Computation

For the microstates of each participant, the following three parameters were computed: (1) the duration of a microstate, which was calculated as the time coverage (in ms) during which all successive original maps were labeled as the same microstate class, starting and ending halfway between the last original map of the preceding microstate and the first original map of the following microstate, respectively; (2) the occurrence rate of a microstate defined as the number of occurrences of a given microstate class per second; (3) the time coverage of a microstate computed as the percentage of occupied total analysis time for a given microstate class (Andreou et al. 2014; Khanna et al. 2014). These three parameters could assess the mean duration, occurrence frequency per second and time coverage of certain underlying large-scale brain networks during resting-state respectively.

Since microstate parameters were evaluated for each epoch separately, the duration of the microstate at the beginning and the end of an epoch was truncated on average of 50%. Corrected duration was computed using the following equation (Schlegel et al. 2012):
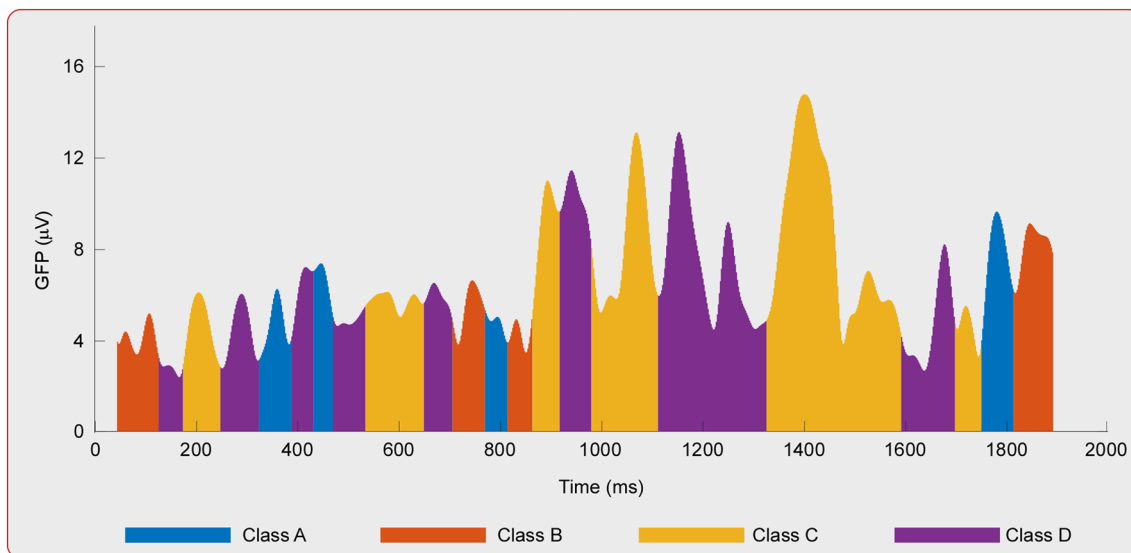
Fig. 1 The microstate sequence of a representative 2000 ms epoch. Fitting the four group-level microstate maps to the original maps revealed that each microstate class appeared repeatedly and domi-

nated during certain time segments, the 'microstates'. These microstates are color-coded in the curve of GFP

$$\text{Duration}_{\text{corrected}} = \frac{\text{duration}_{\text{original}} \times (\text{occurrence} + \text{coverage})}{\text{occurrence}}$$

where $\text{duration}_{\text{corrected}}$ and $\text{duration}_{\text{original}}$ are the corrected and originally computed duration of a microstate class respectively, occurrence is the number of occurrences of this microstate class observed, and coverage is the fraction of time covered by this microstate.

Statistical Analysis

Separate two-way analyses of covariance (ANCOVAs) were performed for the three microstate parameters. Each ANCOVA contained one between-subject factor for group (ASD group and control group), one within-subject factor for microstate classes, and one covariate for age of two groups, since previous study suggested that these parameters may be modulated by age (Koenig et al. 2002). When the main effects or interaction were significant, post-hoc t tests with *age* as covariate were conducted. In order to minimize the risk of type I error, false discovery rate (FDR) correction was applied. The threshold for significance was $p < 0.05$ for the ANCOVAs and the alpha value for FDR procedures was 0.05.

Topographical randomization test was used to test whether the spatial configuration of each microstate class was significantly altered in ASD group (Koenig et al. 1999). More details about this test can be seen in previous literatures (Gao et al. 2017).

In order to further valid the results of topographical randomization tests, the source analysis of each microstate class was conducted separately. The source activities of each microstate class and each participant were estimated using the standardized low-resolution brain electromagnetic tomography (sLORETA), which could calculate the intracerebral electrical source activities from the scalp electrical potentials measured at the electrode sites (Pascual-Marqui 2002). Through the public available LORETA software (http://www.uzh.ch/keyinst/loreta.htm), the neuronal activities in current density (A/m^2) of 6239 cortical gray matter voxels with 5 mm spatial resolution using the MNI152 template were obtained for each microstate class and each participant (Hata et al. 2016). After the source activities of each microstate class and each participant were estimated, voxel-by-voxel permutation based t tests with multiple comparisons correction were conducted to assess the group differences (ASD group vs. control group) regarding current density for each microstate class separately.

Results

We found that in the individual level, the number of optimal clusters varies from 4 to 7 (mean ± SD: 4.93 ± 0.96) for the ASD group, whereas the number of optimal clusters varies from 4 to 7 (mean ± SD: 5.33 ± 1.46) for the control group. In the group level, the optimal cluster number is 4 for both groups. In order to conduct further statistical tests on microstate parameters, microstate class number of each subject was determined to be 4. Here, the four microstate classes

accounted for a mean of 78.60% (SD = 2.67%) and 78.11% (SD = 3.08%) of the data variance across ASD and control group, respectively. The topographies of the four microstate classes of ASD group and control group, which highly resemble those obtained in previous researches, are displayed in Fig. 2 (Britz et al. 2014; Koenig et al. 2002). Thus they were labeled as microstate class A–D in accordance with these studies. Microstate class A, B, C and D exhibit left–right orientation, right–left orientation, anterior–posterior orientation and fronto–central maximum respectively. The topographical randomization tests which could assess whether the spatial distribution of underlying sources was altered showed that the map configuration differed significantly between the two groups for microstate class D ($p < 0.001$). Moreover, significant differences regarding the source activities between ASD and healthy controls were only observed for microstate class D (extreme $p = 0.003$), with patients exhibiting significantly higher activity than controls in right middle frontal gyrus and right superior frontal gyrus (see Table 1).

For microstate occurrence rate, the ANCOVA found that (1) the main effect of microstate class was not significant, $F(3, 90) = 4.02$, $p > 0.05$, $\eta_p^2 = 0.12$; (2) the main effect of group was not significant, $F(1, 30) = 1.70$, $p > 0.05$, $\eta_p^2 = 0.05$; (3) the interaction effect was significant, $F(3, 90) = 7.67$, $p < 0.001$, $\eta_p^2 = 0.20$. Post-hoc tests found that class B and D were significantly more frequent in ASD group compared to control group after FDR correction (Table 2).

The ANCOVA on microstate duration yielded a significant interaction effect, $F(3, 90) = 6.10$, $p < 0.01$, $\eta_p^2 = 0.17$. Post-hoc tests revealed that the durations of class A and class C in control group were significantly longer than those in ASD group (Table 2). There were no significant main effects ($Fs < 2$, $p > 0.05$).

For microstate time coverage, the main effect of microstate class was not significant ($F(3, 90) = 2.63$, $p > 0.05$, $\eta_p^2 = 0.08$). The main effect of group was significant ($F(1, 30) = 4.21$, $p < 0.05$, $\eta_p^2 = 0.12$). The interaction between these two factors was significant ($F(3, 90) = 7.16$, $p < 0.001$, $\eta_p^2 = 0.19$). Follow-up t tests indicated significant differences in the time coverage of class B and C for control group compared to ASD group after FDR correction (Table 2).
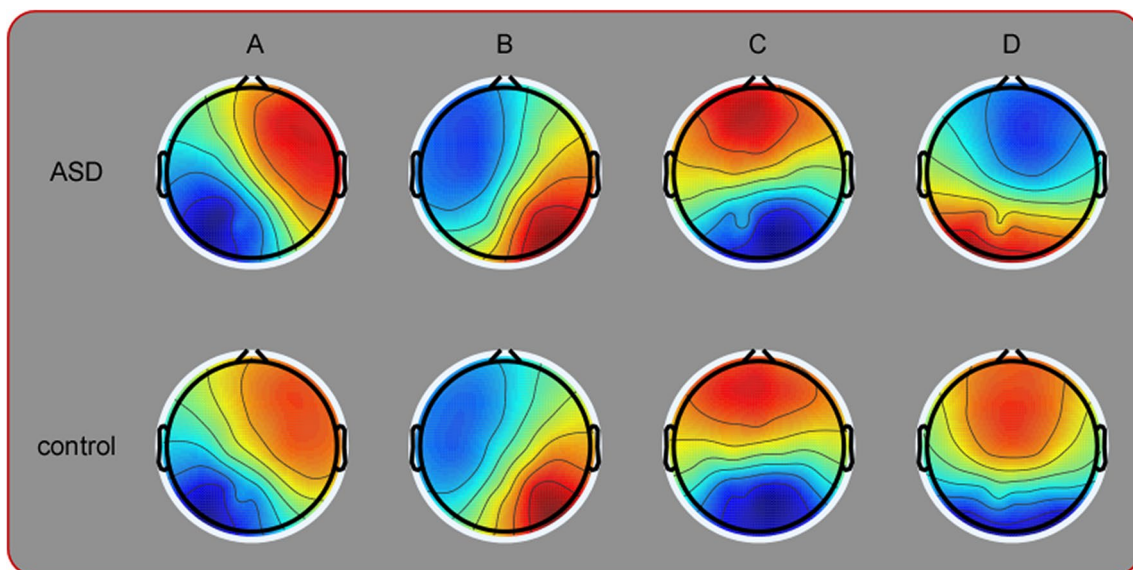
Table 1 The MNI coordinates of voxels with significant group effect (ASD group > control group) for microstate class D and the cortical structures they belong to

x	y	z	Brodmann area	Lobe	Structure
35	30	35	9	Frontal lobe	Middle frontal gyrus
35	35	35	9	Frontal lobe	Superior frontal gyrus
40	30	35	9	Frontal lobe	Middle frontal gyrus
40	35	35	9	Frontal lobe	Superior frontal gyrus
45	35	35	9	Frontal lobe	Middle frontal gyrus
35	30	40	9	Frontal lobe	Middle frontal gyrus
35	35	40	9	Frontal lobe	Middle frontal gyrus
40	30	40	9	Frontal lobe	Middle frontal gyrus
40	35	40	9	Frontal lobe	Superior frontal gyrus
45	30	40	9	Frontal lobe	Middle frontal gyrus
40	30	45	9	Frontal lobe	Middle frontal gyrus
35	25	35	9	Frontal lobe	Middle frontal gyrus

Fig. 2 The group-level maps of the four microstate classes (**a**–**d**) in the ASD group (n = 15) and control group (n = 18)

Table 2 Microstate parameters of the patients with ASD (n = 15) and healthy controls (n = 18)

| | Microstate classes | | | | | | | | |
| | A | | B | | C | | | D | |
	Mean	SD	Mean	SD	Mean	SD		Mean	SD
Occurrence/s									
ASD	3.61	0.54	3.74	0.36	3.46	0.50	3.99		0.55
Control	3.56	0.49	3.19	0.48	3.50	0.44	3.55		0.35
t (df = 31)	− 0.162		− 3.538		0.622		− 2.633		
p	0.873		**0.001**		0.539		**0.013**		
Duration (ms)									
ASD	71.85	7.64	73.76	9.39	71.75	9.17	76.69		8.23
Control	79.57	6.25	74.20	7.26	82.01	8.20	79.93		11.33
t (df = 31)	2.960		0.017		3.295		0.652		
p	**0.006**		0.986		**0.002**		0.519		
Coverage (%)									
ASD	23.86	3.12	25.33	3.46	22.89	3.27	27.91		3.48
Control	25.84	3.27	21.91	3.81	26.21	4.06	26.04		4.75
t (df = 31)	1.708		− 2.688		2.821		− 1.403		
p	0.098		**0.012**		**0.008**		0.171		

Bold values indicate statistical significance after FDR control

Discussion

The present study aimed to investigate resting-state EEG microstates in patients with ASD compared to healthy controls, which may provide some insights into the aberrant intrinsic activities in autistic brain. Consistent with our hypothesis, the spatial and temporal properties of certain microstate classes were found to be altered in our patient sample. Although this is only a preliminary study, it clearly indicates that the resting-state EEG microstate analysis may provide indices that can be used in the ASD researches.

The Functional Significance of EEG Microstate Class

The functional significance of these microstate classes have been explored for decades, and some consensuses have been reached (Britz et al. 2010; Khanna et al. 2014; Michel and Koenig 2017). Microstate class A was found correlated with negative BOLD activations in bilateral superior and middle temporal gyri which were crucial in phonological processing (Britz et al. 2010). Microstate class B was suggested to reflect the visual resting state networks and involved in imagery thoughts (Britz et al. 2010; Lehmann et al. 1998). Although the physiological basis of microstate class C is still highly debated, this microstate class was believed to be associated with the anterior default mode network, which could integrate interoceptive information with emotional salience in order to form a subjective representation of the own body (Michel and Koenig 2018; Taylor et al. 2009). The last microstate class (class D) is associated with activities in lateralized dorsal and ventral areas of frontal and parietal cortex, which were part of the dorsal attention network (Britz et al. 2010).

Altered Temporal and Spatial Properties in Patients with ASD

Firstly, we found that the durations of phonological processing related class A and self-representation related class C in ASD group were significantly shorter than those in control group. One of the key characteristics in ASD is impairments in social communicative development (Amaral et al. 2008). Moreover, impairments in phonological processing ability and atypical neural representation of the self could result in the communication deficits in patients with ASD and are keys to understanding the nature of ASD (Anderson et al. 2010; Eyler et al. 2012). The current study highlighted that these impairments may be caused by the fact that the phonological processing and self-representation related cognitive processes might terminate prematurely in patients with ASD, thus these patients do not have enough time so as to adequately process related external or internal information.

Secondly, we found that the occurrence rate and time coverage of the visual network related class B in ASD group were significantly larger than those in control group. A commonly observed associated feature of the autistic phenotype is atypical perceptual processing ability, often manifested as enhanced perceptual performance (Samson et al. 2012). To account for these findings, the enhanced perceptual functioning model (EPFM) proposes that enhanced autistic

performance in basic perceptual tasks results from stronger engagement of sensory processing mechanisms, a situation that may facilitate an atypically prominent role for perceptual mechanisms in supporting cognition (Mottron et al. 2006). We found that this visual processing related network occurred more frequently and occupied more time in patients with ASD, even during task-free resting state. Thus, our findings could be seen as evidence in support of the EPFM.

Thirdly, as for microstate class D, the occurrence rate in ASD group was significantly larger than that in control group. Furthermore, the map configuration of microstate class D in ASD group was significantly different from that in control group, which suggested that the underlying brain network of class D of ASD group was different from that of controls. Further source analysis revealed that the areas exhibiting significant group differences (ASD group > control group) for microstate class D located in right frontal lobe, especially right middle frontal gyrus. This region is considered to be part of the ventral attention network (VAN), and is involved in different aspects of bottom-up attention (e.g., reorienting to unexpected stimuli) (Shulman et al. 2010). This is consistent with the functional significance of microstate class D, and previous studies which revealed that functional abnormality in the frontal regions was central in autism and its abnormality could contribute to the dysfunction in individuals' behavior development (Li and Yu 2016; Shalom 2009). Thus, such a result confirmed again the importance of the right frontal regions in ASD.

With respect to the results of the current study, at least three points need to be mentioned. Firstly, most previous studies in the field of EEG microstate analysis used eye-closed resting-state EEG signals. However, in the current study, the EEG signals have mixed eye-open and eye-closed time periods. It has been well known that many EEG measures (including the microstate temporal parameters) could be significantly altered in eye-open condition, compared with those in eye-closed condition. Secondly, the mean duration and time coverage of microstate class C of control group were larger than those of the other microstate classes. The pattern of control group is similar to that reported in previous studies using EEG datasets of participants in childhood and adolescence (Tomescu et al. 2018). Note that, this trend is absent in ASD group. This puzzling result may be caused by the following reasons: (1) the EEG signals being investigated had mixed eye-open and eye-closed time periods; (2) the neuropathological condition (i.e., ASD) may significantly influence the main effects of the temporal parameters of four microstate classes. Thirdly, the ages of participants in control group were much younger than those of participants in ASD group. Previous studies revealed that the temporal parameters could be significantly influenced by the age of participants, e.g., prolong duration of microstate class C from childhood to adolescence (Tomescu et al. 2018). Note

that, the mean age of ASD participants was larger than that of controls, and the mean duration of microstate class C was shorter in ASDs, which suggested that the results observed here should not be produced by the age difference between two groups, and may indicate some kinds of developmental lag which have been proved by dozens of studies (Schover and Newsom 1976; Williams et al. 2013).

Comparison with Other Diseases

Ever since the development of EEG microstate technique, it has been applied to numerous studies, which investigated the alterations of EEG microstate parameters in patients with neuropsychiatric diseases (Andreou et al. 2014; Gao et al. 2017; Michel and Koenig 2018; Rieger et al. 2016). Perhaps, the most frequently investigated disorder using this method is schizophrenia. A meta-analysis on studies of recent years confirmed that the temporal parameters of microstate class C and D are closely associated with schizophrenia, i.e., patients with schizophrenia exhibited significantly larger occurrence rate of microstate class C and shorter duration of microstate class D (Rieger et al. 2016). Moreover, the altered microstate parameters can be used to detect the vulnerability of patients at risk for schizophrenia and the effects of treatment (Kikuchi et al. 2007; Tomescu et al. 2015). In the current study, we found that in ASD group, the duration of class C was significantly shorter and the occurrence rate of class D was significantly larger. These results suggest that although both diseases (i.e., schizophrenia and ASD) could modulate the temporal parameters of microstate class C and D, they may influence distinct aspects of underlying cortical networks.

In this study, altered temporal parameters were also observed for microstate class A and class B. Investigation on some other diseases (e.g., multiple sclerosis, narcolepsy and spastic diplegia) also revealed significantly class A and B temporal parameters (Drissi et al. 2016; Gao et al. 2017; Gschwind et al. 2016), which indicated that lower-order sensory networks were affected in these disorders. It's interesting that both lower-order sensory networks (reflected by microstate class A and B) and higher-level cognitive networks (reflected by microstate class C and D) were modulated by ASD.

Limitations of the Current Study

Although the current study suggested that resting-state EEG microstate analysis could provide important measures that could be used in ASD researches, it at least has the following two limitations. As has been illustrated above, the first limitation is that the EEG signals being investigated have mixed eye-open and eye-closed time periods. The microstate parameters may be significantly altered in eye-open condition,

compared with those in eye-closed condition. We did not conduct microstate analysis on eyes open epochs and eyes closed epochs respectively, since this will result in noisy topographical maps of microstate classes with low SNR which may be caused by the relatively small number of both kinds of epochs. We believed that the paradigm used in current study (i.e., resting state EEG recording with alternating eyes open and eyes closed periods) was more convenient for ASD researches, since those patients with ASD were unwilling to keep eyes open or eyes closed for a relatively long time (e.g., 5 min). For these practical reasons, we decided to conduct microstate analysis on both kinds of epochs. The second limitation of the current study is that the age range (i.e., from 5 to 18 years old) is relatively large. In the future, we should enlarge the sample size, and investigate whether some demographic variables (e.g., age, sex and comorbidities) could modulate the spatial and temporal microstate parameters in patient with ASD.

Conclusions

Here, the aberrant intrinsic brain activity in patients with ASD was investigated using parameters of resting-state microstate classes, which provided new insights into the neuropathological mechanisms in ASD. The occurrence rate and time coverage of visual network related microstate class B, the duration of phonological processing related microstate class A, the duration and time coverage of self-representation related microstate class C, and the map configuration and occurrence rate of the dorsal attention network related microstate class D were significantly altered in ASD group. This study clearly indicated that the resting-state EEG microstate analysis may provide biomarkers that can be used in clinical researches of ASD.

Compliance with Ethical Standards

Conflict of interest The authors declare that they have no conflict of interests.

Ethical Approval All procedures performed in studies involving human participants were in accordance with the ethical standards of the institutional and/or national research committee and with the 1964 Helsinki declaration and its later amendments or comparable ethical standards.

References

Alexander LM et al (2017) An open resource for transdiagnostic research in pediatric mental health learning disorders. Sci Data 4:170181

Amaral DG, Schumann CM, Nordahl CW (2008) Neuroanatomy of autism. Trends Neurosci 31:137–145

Anderson JS et al (2010) Decreased left posterior insular activity during auditory language in autism. Am J Neuroradiol 31:131–139

Andreou C et al (2014) Resting-state connectivity in the prodromal phase of schizophrenia: insights from EEG microstates. Schizophr Res 152:513–520

Britz J, Van De Ville D, Michel CM (2010) BOLD correlates of EEG topography reveal rapid resting-state network dynamics. Neuroimage 52:1162–1170

Britz J, Díaz HL, Ro T, Michel CM (2014) EEG-microstate dependent emergence of perceptual awareness. Front Behav Neurosci 8:163–163

Brunet D, Murray MM, Michel CM (2010) Spatiotemporal analysis of multichannel EEG: CARTOOL. Comput Intell Neurosci 2011:813870

Chen H, Nomi JS, Uddin LQ, Duan X, Chen H (2017) Intrinsic functional connectivity variance and state-specific under-connectivity in autism. Hum Brain Mapp 38:5740–5755

Delorme A, Makeig S (2004) EEGLAB: an open source toolbox for analysis of single-trial EEG dynamics including independent component analysis. J Neurosci Methods 134:9–21

Drissi NM et al (2016) Altered brain microstate dynamics in adolescents with narcolepsy. Front Hum Neurosci 10:369

Eyler LT, Pierce K, Courchesne E (2012) A failure of left temporal cortex to specialize for language is an early emerging and fundamental property of autism. Brain 135:949

Falahpour M et al (2016) Underconnected, but not broken? Dynamic functional connectivity MRI shows underconnectivity in autism is linked to increased intra-individual variability across time. Brain Connect 6:403–414

Gao F, Jia H, Wu X, Yu D, Feng Y (2017) Altered resting-state EEG microstate parameters and enhanced spatial complexity in male adolescent patients with mild spastic diplegia. Brain Topogr 30:233–244

Gschwind M et al (2016) Fluctuations of spontaneous EEG topographies predict disease state in relapsing-remitting multiple sclerosis. Neuroimage Clin 12:466–477

Hata M et al (2016) Functional connectivity assessed by resting state EEG correlates with cognitive decline of Alzheimer's disease—an eLORETA study. Clin Neurophysiol 127:1269–1278

Jung M et al (2014) Default mode network in young male adults with autism spectrum disorder: relationship with autism spectrum traits. Mol Autism 5:35

Just MA, Cherkassky VL, Keller TA, Minshew NJ (2004) Cortical activation and synchronization during sentence comprehension in high-functioning autism: evidence of underconnectivity. Brain 127:1811–1821

Just MA, Keller TA, Malave VL, Kana RK, Varma S (2012) Autism as a neural systems disorder: a theory of frontal-posterior underconnectivity. Neurosci Biobehav Rev 36:1292–1313

Kaufman J et al (1997) Schedule for affective disorders and schizophrenia for school-age children-present and lifetime version (K-SADS-PL): initial reliability and validity data. J Am Acad Child Adolesc Psychiatry 36:980–988

Khanna A, Pascual-Leone A, Michel CM, Farzan F (2014) Microstates in resting-state EEG: current status and future directions. Neurosci Biobehav Rev 49:105–113

Kikuchi M, Koenig T, Wada Y, Higashima M, Koshino Y, Strik W, Dierks T (2007) Native EEG and treatment effects in neuroleptic-naive schizophrenic patients: time and frequency domain approaches. Schizophr Res 97:163–172

Koenig T, Lehmann D, Merlo MCG, Kochi K, Hell D, Koukkou M (1999) A deviant EEG brain microstate in acute, neuroleptic-naive schizophrenics at rest. Eur Arch Psychiatry Clin Neurosci 249:205–211

Koenig T et al (2002) Millisecond by millisecond, year by year: normative EEG microstates and developmental stages. Neuroimage 16:41–48

Lehmann D, Strik WK, Henggeler B, Koenig T, Koukkou M (1998) Brain electric microstates and momentary conscious mind states as building blocks of spontaneous thinking: I. Visual imagery and abstract thoughts. Int J Psychophysiol 29:1–11

Lehmann D et al (2005) EEG microstate duration and syntax in acute, medication-naive, first-episode schizophrenia: a multi-center study. Psychiatry Res 138:141–156

Li Y, Yu D (2016) Weak network efficiency in young children with autism spectrum disorder: evidence from a functional near-infrared spectroscopy study. Brain Cogn 108:47–55

Lord C, Rutter M, DiLavore PC, Risi S, Gotham K, Bishop S (2012) Autism Diagnostic Observation Schedule—second edition (ADOS-2). Western Psychological Corporation, Torrence

Michel CM, Koenig T (2018) EEG microstates as a tool for studying the temporal dynamics of whole-brain neuronal networks: a review. Neuroimage 180:577–593

Mottron L, Dawson M, Soulières I, Hubert B, Burack J (2006) Enhanced perceptual functioning in autism: an update, and eight principles of autistic perception. J Autism Dev Disord 36:27–43

Murray MM, Brunet D, Michel CM (2008) Topographic ERP analyses: a step-by-step tutorial. Rev Brain Topogr 20:249–264

Oldfield RC (1971) The assessment and analysis of handedness. Edinb Inventory Neuropsychol 9:97–113

Parellada M, Penzol MJ, Pina L, Moreno C, González-Vioque E, Zalsman G, Arango C (2014) The neurobiology of autism spectrum disorders. Eur Psychiatry 29:11–19

Pascual-Marqui RD (2002) Standardized low-resolution brain electromagnetic tomography (sLORETA): technical details. Methods Find Exp Clin Pharmacol 24:5–12

Pascual-Marqui RD, Michel CM, Lehmann D (1995) Segmentation of brain electrical activity into microstates: model estimation and validation. IEEE Trans Biomed Eng 42:658–665

Rieger K, Diaz Hernandez L, Baenninger A, Koenig T (2016) 15 Years of microstate research in schizophrenia—Where are we? A meta-analysis. Front Psychiatry 7:22

Samson F, Mottron L, Soulières I, Zeffiro TA (2012) Enhanced visual functioning in autism: an ALE meta-analysis. Hum Brain Mapp 33:1553–1581

Santarnecchi E et al (2017) EEG microstate correlates of fluid intelligence and response to cognitive training. Brain Topogr 30:502–520

Schlegel F, Lehmann D, Faber PL, Milz P, Gianotti LRR (2012) EEG microstates during resting represent personality differences. Brain Topogr 25:20–26

Schover LR, Newsom CD (1976) Overselectivity, developmental level, and overtraining in autistic and normal children. J Abnorm Child Psychol 4:289–298

Seitzman BA, Abell M, Bartley SC, Erickson MA, Bolbecker AR, Hetrick WP (2017) Cognitive manipulation of brain electric microstates. Neuroimage 146:533–543

Shalom DB (2009) The medial prefrontal cortex and integration in autism. Neuroscientist 15:589–598

Shulman GL, Pope DLW, Astafiev SV, Mcavoy MP, Snyder AZ, Corbetta M (2010) Right hemisphere dominance during spatial selective attention and target detection occurs outside the dorsal frontoparietal network. J Neurosci 30:3640–3651

Taylor KS, Seminowicz DA, Davis KD (2009) Two systems of resting state connectivity between the insula and cingulate cortex. Hum Brain Mapp 30:2731–2745

Tomescu MI et al (2015) Schizophrenia patients and 22q11.2 deletion syndrome adolescents at risk express the same deviant patterns of resting state EEG microstates: a candidate endophenotype of schizophrenia. Schizophr Res Cogn 2:159–165

Tomescu MI et al (2018) From swing to cane: sex differences of EEG resting-state temporal patterns during maturation and aging. Dev Cogn Neurosci 31:58–66

Van de Ville D, Britz J, Michel CM (2010) EEG microstate sequences in healthy humans at rest reveal scale-free dynamics. Proc Natl Acad Sci USA 107:18179–18184

Williams DL, Goldstein G, Minshew NJ (2013) The modality shift experiment in adults and children with high functioning autism. J Autism Dev Disord 43:794–806

Woolfenden S, Sarkozy V, Ridley G, Williams K (2012) A systematic review of the diagnostic stability of autism spectrum disorder. Res Autism Spectr Disord 6:345–354